Forest Ecology and Management 457 (2020) 117727

Contents lists available at ScienceDirect

Forest Ecology and Management

journal homepage: www.elsevier.com/locate/foreco

Transference of *Robinia pseudoacacia* water-use patterns from deep to shallow soil layers during the transition period between the dry and rainy seasons in a water-limited region

Yali Zhao[a,d,e], Yunqiang Wang[a,b,c,d,f,*], Meina He[a], Yongping Tong[a], Jingxiong Zhou[a], Xiangyu Guo[a,d], Jinzhao Liu[a,b], Xingchang Zhang[d,e]

[a] State Key Laboratory of Loess and Quaternary Geology, Institute of Earth Environment, Chinese Academy of Sciences, Xi'an, Shaanxi 710061, China
[b] CAS Center for Excellence in Quaternary Science and Global Change, Xian 710061, China
[c] Interdisciplinary Research Center of Earth Science Frontier, Beijing Normal University, Beijing 100875, China
[d] Graduate University of Chinese Academy of Sciences, Beijing 100049, China
[e] State Key Laboratory of Soil Erosion and Dryland Farming on the Loess Plateau, Institute of Soil and Water Conservation, Chinese Academy of Sciences & Ministry of Water Resources, Yangling 712100, China
[f] Department of Earth and Environmental Sciences, Xi'an Jiaotong University, Xi'an 710049, China

ARTICLE INFO

Keywords:
Stable isotopes
Robinia pseudoacacia
Water uptake pattern
Dried soil layer
The Loess Plateau

ABSTRACT

Soil water plays a critical role in determining plant survival and growth globally, especially in water-limited regions. This study explores water-use characteristics of *Robinia pseudoacacia* during the transition period between the dry and rainy seasons in the Chinese Loess Plateau (CLP). A stable isotope technique ($\delta^{18}O$ and δD) and two complementary approaches (i.e., the direct inference method and the MixSIAR model) were used to distinguish water source changes during this transition period. Based on $\delta^{18}O$ and δD distribution patterns, we subdivided a 500 cm soil profile into four potential water sources: shallow (0–40 cm), intermediate-shallow (40–120 cm), intermediate (120–200 cm) and deep (200–500 cm). During the transition period, *R. pseudoacacia* exhibited different water uptake patterns. In April 26.2% and 48.4% of water uptake derived from the 40 to 120 and 200 to 500 cm soil profile layers; in May, 21.5%, 24.5% and 37.4% of water was absorbed from the 0 to 40, 40 to 120 and 200 to 500 cm soil profile layers. In June and July, 51.6% and 53.6% of the water mainly derived from the 0 to 120 cm soil profile layer, respectively. During the dry season (April), the trend in water uptake shifted to the deep soil layer, potentially a key period for the onset of soil desiccation in this soil layer. As precipitation increased, the proportion of water uptake from the shallow and intermediate-shallow soil layers increased. Because water-use pattern characteristics could provide important information on the development of the dried soil layer (DSL), the stable isotope technique could help reveal the water sources used by trees while also offering insight into water movement mechanisms of local ecosystems. Given its usefulness, the application of the stable isotope technique should be expanded in analyzing practical ecohydrological issues that occur in deep soils in the future.

1. Introduction

Soil water plays a critical role in the survival and growth of plants. In water-limited regions, the availability of soil water will likely decline under a warming climate and a decrease in precipitation, which is predicted by most general circulation models (Schuur et al., 2008; Leo et al., 2014). Furthermore, climate change has increased the intensity and duration of seasonal drought periods, which has decreased overall growth-plant habitats and threatened plant survival in water-deficit ecosystems (Barbeta et al., 2015). Plants must therefore adapt to water shortages throughout their life cycles by adjusting how they utilize various available water sources (Matzner et al., 2003; Zhang et al., 2010; Wesche et al., 2011; Su et al., 2014). Accordingly, investigating the water-use pattern of plants is necessary to improve our knowledge of plant survival strategies and to understand plant mechanisms in response to drought in water-limited regions.

* Corresponding author at: State Key Laboratory of Loess and Quaternary Geology, Institute of Earth Environment, Chinese Academy of Sciences, Xi'an, Shaanxi 710061, China.
E-mail address: wangyunq04@163.com (Y. Wang).

https://doi.org/10.1016/j.foreco.2019.117727
Received 20 June 2019; Received in revised form 25 October 2019; Accepted 25 October 2019
Available online 04 December 2019
0378-1127/

The stable isotope technique ($\delta^{18}O$ and δD) has developed into a powerful tool for investigating relationships during plant-water processes, such as understanding how plant water-use strategies respond to different types of water sources, as well as providing a better understanding of water utilization processes, water-use efficiency, patterns, mechanisms and the ability of plants to adapt to semiarid and arid environments (Ehleringer and Dawson, 1992; Asbjornsen et al., 2008; Lubis et al., 2014). Generally, the isotopic composition of both hydrogen and oxygen in water does not alter when absorbed by roots and transported from roots to shoots (Ehleringer and Dawson, 1992; Ellsworth and Williams, 2007). Thus, the specific source of water that is absorbed by plant roots can be confirmed by comparing hydrogen and oxygen isotopes extracted from plant xylem and probable water sources. There are also marked differences between $\delta^{18}O$ and δD in various types of water bodies due to varying water cycles, making it possible to identify plant water sources and to determine the utilization regime of various potential water sources (Corbin et al., 2005; Lubis et al., 2014).

Numerous studies have described plant water uptake patterns in semiarid and arid habitats by applying the $\delta^{18}O$ and δD isotope technique. For example, trees, shrubs and grasses are able to coexist in savanna communities because trees and shrubs generally tend to use deep water sources while grasses tend to use shallow water sources, a pattern that correlates to the different root distribution patterns of these plants (Walker et al., 1981; Sala et al., 1989; Scholes and Archer, 1997; House et al., 2003). In a semiarid sandy region of Northwest China, for example, it has been shown that *Pinus sylvestris* var. *mongolica* utilizes soil water in spring (April–May) and autumn (September–October), while it utilizes both soil water and groundwater in summer (June–August) (Song et al., 2016b). Using *P. sylvestris* var. *mongolica* as a afforestation species in this sandy region to prevent and control desertification has caused irreversible groundwater loss, and older trees may experience an increase in mortality in the future if groundwater levels suddenly decline under drought conditions (Song et al., 2016a). Generally, the water-use patterns of plants are affected by various physiological and physical characteristics, such as (1) the distribution and function of fine roots: deep-rooted species can utilize deeper soil water and groundwater than shallow-rooted species under water-stress conditions (Nie et al., 2011; Wu et al., 2017); (2) water availability: trees that grow in semiarid and arid regions uptake most source water from shallow soil layers during the rainy season but later shift to uptake more water from deeper soil layers (wherein the largest depths are typically < 2 m) or groundwater during the dry season (Nie et al., 2011; Dai et al., 2015); (3) water demands of trees: mature trees may require more water to meet their transpiration needs compared to younger trees (Eggemeyer et al., 2009; Kerhoulas et al., 2013), which is associated with the leaf area index (LAI), biomass, the vapor pressure deficit (VPD), etc.

The Chinese Loess Plateau (CLP) is typical of water-limited ecosystems found throughout the world. The region is characterized by a thick loess deposit, which ranges from 30 to 80 m (Yang and Gao, 1998; Chen et al., 2008a). *Robinia pseudoacacia* (*R. pseudoacacia*) has become a predominant species cultivated in the CLP following the implementation of the Grain for Green program, which was widely supported by numerous scientists, land managers and policymakers. It was reported that by 2008 total vegetation restoration reached 4.83 Mha in the CLP (Chen et al., 2015), wherein *R. pseudoacacia* is estimated to currently populate half of the total area. During the past decade, some studies reported that intensive vegetation restoration over large areas may aggravate soil water scarcity and lead to soil desiccation in the soil profile (Chen et al., 2008b; Wang et al., 2008, 2018). Soil desiccation will further cause the formation of a dried soil layer (DSL). It is important to note that DSLs can profoundly hinder hydrological cycles within a soil-vegetation atmosphere system by blocking water exchange between the aeration zone and groundwater, which may lead to poor soil water availability while also undoing the ecological successes that have already been achieved (Wang et al., 2010, 2011). Previous studies have reported that the water consumption of *R. pseudoacacia*, being an exotic species in China, is highest compared to local shrubs and grasses in the CLP, which in turn has intensified soil desiccation (Shangguan, 2007; Wang et al., 2008, 2015). Furthermore, the transition period from the dry to the rainy season is a crucial stage in plant development when they revive from dormancy, which follows a substantial increase in both temperature and rainfall. With such a drastic change in the external environment and the soil environment, it may be inferred that plants will correspondingly react to this transformation by altering the intrinsic physiology of their water uptake mechanisms.

To the best of our knowledge, only limited effort has been made to explore water uptake strategies of *R. pseudoacacia* following the formation of DSLs and, consequently, the relationship between DSL evolution and the water-use strategy of *R. pseudoacacia*. Moreover, information on *R. pseudoacacia* water-use strategies during this transition period (from the dry to the rainy season) remains unclear. Although studies have been conducted in the CLP to investigate water-use patterns of other species by using the stable isotope technique, soil profile data from these studies were limited to 200 cm (Wan and Liu, 2016; Huo et al., 2018). Furthermore, the roots of *R. pseudoacacia* can reach into the very deep strata of the soil profile (Li et al., 2018); therefore, these roots can absorb deep soil water to meet survival and growth demands, which may in turn affect the extent of DSL development. However, isotopic signatures of hydrogen and oxygen (δD and $\delta^{18}O$, respectively) have not been clarified in these deep soil layers. Further data on *R. pseudoacacia* water-use characteristics in the deep soil layer is therefore necessary to better understand water movement in the soil-vegetation atmosphere system and to determine the development of DSLs.

Accordingly, the objectives of this study were (1) to investigate the distribution patterns of soil and plant root properties in a 0–500 cm soil profile after DSL formation in the CLP; (2) to ascertain *R. pseudoacacia* water-use strategy characteristics in this 500 cm soil profile during the transition period from the dry to the rainy season; and (3) to reveal the impact that such water-use strategies have on the development of DSLs.

2. Materials and methods

2.1. Study area

This study was conducted in the Gutun watershed, located in the middle of the CLP (Fig. 1). Characteristic climate conditions are as follows: a mean annual temperature of 9.8 °C, a mean annual precipitation of 541 mm and a relatively high pan evaporation of 1000 mm (Wang et al., 2008), experiencing a long cold winter. The study area is mainly composed of wind-deposited loess soil with low fertility which is weakly resistant to erosion. Commencing in 2003, the watershed has recovered under the auspice of the Grain for Green program. Common vegetation species in the watershed are black locust (*Robinia pseudoacacia* L.), korshinsk pea shrub (*Caragana korshinskii* Kom.), sea buckthorn (*Hippophae rhamnoides* L.) and bungeneedle grass (*Stipa bungeana* Trin.). *R. pseudoacacia* is the predominant tree species in the watershed, with a total coverage rate of 60%~75%.

2.2. Sample collection

Our field experiment was conducted on a typical slope in the Gutun watershed covered by *R. pseudoacacia* trees planted in 2003 (being 16 yr old at the time of this study). Three 10 m × 10 m plots (used as three replicates) were established as the permanent field sites in our study. To determine soil particle composition and monitor dynamics of soil water content (SWC), we used a soil auger (5 cm in diameter) with five auxiliary drill pipes (each drill pipe being 1-m in length) to collect "disturbed" soil samples (i.e., aggregated soil samples from the different soil layers) to a depth of 500 cm at intervals of 20 cm in each plot.

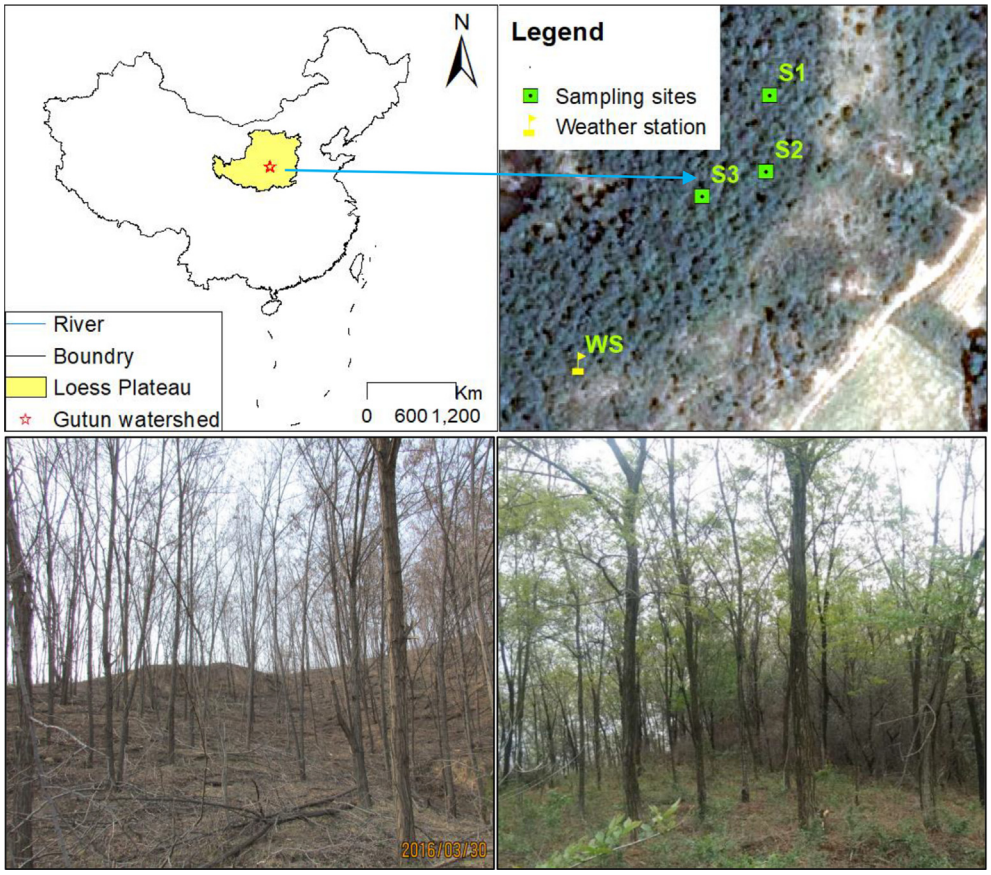

Fig. 1. Location of the Chinese Loess Plateau (CLP) and the sampling sites as well as photographs of *Robinia pseudoacacia* specimens in dry and rainy seasons in the study area.

Following this, an aluminum neutron probe access tube was installed to record SWC at 20 cm intervals from the 0 to 500 cm soil profile. To ascertain the root pattern of *R. pseudoacacia* trees, we collected plant root samples using a soil auger (10 cm in diameter) at 20 cm intervals from the 0 to 200 cm soil profile layer and at 50 cm intervals from the 200–500 cm soil profile layer. In total, we collected 225 soil samples and 144 plant root samples. The disturbed soil samples were air dried and passed through a 1 mm diameter mesh to determine soil particle composition. The roots were washed with water after weighing the fresh weight of roots, then they were air dried for 4 to 8 h and finally scanned on a STD 4800 Scanner. Root length density, root surface area density and average diameter density were obtained using the WinRHIZO image analysis system software package.

To explore the water-use pattern of *R. pseudoacacia* during the transition period from the dry to the rainy season, soil samples and *R. pseudoacacia* twigs were collected from each plot for isotopic analysis in April, May, June and July 2016, respectively. The soil sampling scheme used was similar to that used for roots (i.e., soil auger), and soil was then sealed in individual vials and frozen at –20 ˚C until water extraction was conducted in the laboratory. Five fully suberized twigs taken from lateral branches of *R. pseudoacacia* were sampled for xylem water extraction. To prevent evaporative fractionation, the phloem of each plant sample was removed, and the xylem was immediately placed into individual vials. The vials were then sealed with Parafilm and stored in a freezer at –20 ˚C for isotopic analysis. In general, 48 soil samples and three plant samples were collected during each sampling period.

Precipitation samples were collected through a funnel device which prevented evaporation, and rainfall samples were collected after each rain event between May and August 2016 at a local experimental station. Samples were immediately sealed in screw cap glass vials, which were sealed with Parafilm and refrigerated at 4 ˚C for isotopic analysis. In total, 30 rainwater samples were collected. Meteorological data on precipitation and air temperature were obtained from an automatic weather station (AWS) located approximately 300 m from the plots (Fig. 1).

2.3. Stable isotope analysis

Rainfall samples were filtered to eliminate any impurities before conducting isotopic analysis. A cryogenic vacuum distillation system was used to extract water from soil and plant xylem samples in the laboratory, and the extracted water was stored in screw cap glass vials at 4 ˚C for isotopic determination. The stable isotopic composition ($\delta^{18}O$ and δD) of liquid water was determined using a Picarro L2130-I isotope water analyzer (Sunnyvale, CA, USA) at the State Key Laboratory of Loess and Quaternary Geology, Institute of Earth Environment (IEE), Chinese Academy of Sciences (CAS). Each sample was injected six times, but the first three injections were discarded to eliminate potential memory effects. The average composition for injections 4 through 6 was used to calculate the isotope ratio. Analysis was performed in the following order: three standard samples, six natural samples and three standard samples, which eliminated both memory and drift effects. A previous study already verified that there was no organic contamination in soil water and rain water (Schultz et al., 2011). We used the Micro-Combustion Module (Picarro) to remove organic compounds contaminating water samples from the xylem. The accuracy of the measurements was ± 0.1 (‰) for $\delta^{18}O$ and ± 1 (‰) for δD. The isotopic composition of $\delta^{18}O$ and δD is expressed as an isotope ratio:

$$\delta_{sample}(\%) = \left(\frac{R_{sample} - R_{VSMOW}}{R_{VSMOW}}\right) \times 1000$$

where δ_{sample} is the deviation of the isotope ratio of a sample relative to that of the Vienna Standard Mean Ocean Water (V_{SMOW}); R_{sample} is the ratio of ^{18}O to ^{16}O atoms (or D to H atoms) in the sample; and R_{vsmow} is the ratio of ^{18}O to ^{16}O atoms (or D to H atoms) in the V_{SMOW}.

2.4. Statistical methods

Two methods were used to identify the source of water absorbed by *R. pseudoacacia*. First, isotope ratios of xylem water were compared directly with those of soil water in the vertical profile, a method referred to as "direct inference" (Asbjornsen et al., 2007; Li et al., 2007). Second, the MixSIAR model was used to determine the relative proportion of each water source to *R. pseudoacacia* throughout the four-month study period. The MixSIAR model can estimate the proportion of source contributions to a mixture through options for fixed/random effects, source data types, priors and error terms (Parnell et al., 2013). In this study, the raw xylem isotope values (δD and $\delta^{18}O$) of *R. pseudoacacia* were used as the mixture data inputs into MixSIAR. The raw isotope values (δD and $\delta^{18}O$) from each soil layer were used as source data inputs into MixSIAR. Source data were confirmed to have no concentration dependence. Individual effects and zero discrimination were set in the model. The run length of the Markov chain Monte Carlo (MCMC) was set to "long" (chain length = 300 000; burn = 200 000; thin = 100; chains = 3). The water sources taken from the different soil layers were combined into four layers (0–40, 40–120, 120–200 and 200–500 cm) to facilitate the subsequent analysis and comparison. The four soil layers were identified by the following criteria:

(1) Shallow soil layer (0–40 cm): the isotopic ratios in soil water and SWC showed large variability and were vulnerable to the precipitation pulse and evaporation.
(2) Intermediate-shallow soil layer (40–120 cm): the isotopic ratios in soil water and SWC were variable on a monthly scale and were influenced by infiltration.
(3) Intermediate soil layer (120–200 cm): the isotopic ratios in soil water and SWC showed low variability and weaker monthly changes than the two abovementioned soil layers.
(4) Deep soil layer (200–500 cm): the isotopic ratios in soil water and SWC exhibited relatively stable variations if water use of deep roots was not considered.

Furthermore, we provided DSL distribution, which is defined as a soil layer with SWC being less than the stable field capacity (SFC) according to the method proposed by Wang et al. (2010, 2011). The SFC was equal to 60% of the field capacity (at a water content of −0.03 MPa) according to the soil texture in the study area.

All statistical analyses were performed using Microsoft Excel (version 2013) and SPSS (version 16.0). Maps of sampling points were generated using GIS software (ArcGis version 10.2). The diagrams were generated using Origin version 9 and SigmaPlot version 12.5.

3. Results

3.1. Basic information on soil and plant root properties

3.1.1. Soil particle composition

The distribution of soil particle composition in the 0–500 cm soil profile is shown in Fig. 2A. Clay content was almost entirely uniform across the whole soil profile. Silt and sand content generally showed the reverse trend in that silt content increased while sand content decreased in the 0–60 cm soil profile layer. Statistical analysis of soil particle composition in the four soil profile layers (0–40, 40–120, 120–200 and 200–500 cm) is shown in Table 1. Mean clay content in the four soil profile layers ranged from 3.34% in the 40–120 cm soil profile layer to 3.88% in the 200–500 cm soil profile layer. Mean silt content increased from 64.91% in the 0–40 cm soil profile layer to 74.23% in the 200–500 cm soil profile layer, while mean sand content decreased from 31.27% in the 0–40 cm soil profile layer to 21.89% in the 200–500 cm soil profile layer. The standard deviation (SD) of soil particle composition in the upper soil profile layer was higher relative to the deep soil profile layer. This was also the case for the coefficient of variation (CV).

3.1.2. Plant roots

All four root parameters decreased in the 0–200 cm soil profile layer and then stabilized in the 200–500 cm soil profile layer (Fig. 2B). Fine root distribution patterns were similar (Fig. 2C). Table 1 lists the statistical data of the four root parameters. The mean root length density varied from 0.038 to 0.493 cm/cm^3, and the mean root surface area density ranged from 0.004 to 0.056 cm^2/cm^3. The mean root average diameter decreased from 0.324 to 0.083 $mm/cm^3 \times 10^{-3}$ with an increase in the depth of the soil profile. The mean root weight decreased from 0.937 in the 0–40 cm soil profile layer to 0.041 g/cm^3 in the 200–500 cm soil profile layer. Contrary to soil particle composition, the CV of plant roots showed an increasing trend with an increase in soil depth except for the 40–120 cm soil profile layer. Compared to the whole profile, root biomass percentages in the 0–120 cm soil profile layer for root length density, root surface area density, root average diameter density and root weight density were 84%, 79%, 42% and 85%, respectively, which indicated that the majority of plant roots were distributed in the shallow soil profile layer.

3.1.3. Soil water content and the dried soil layer phenomenon

Monthly SWC within the 0–500 cm soil profile layer and mean SWC within the 200–500 cm soil profile layer are shown in Fig. 3. The four SWC measurements showed large variation in the 0–160 cm soil profile layer but was stable (7–8%) in the deep soil profile layer. The SWC for April and May peaked at 60 cm and then decreased with increasing soil depth. Furthermore, the SWC for June and July was lower than for April and May in the 0–150 cm soil profile layer. Statistical SWC values of the four soil profile layers (i.e., 0–40, 40–120, 120–200 and 200–500 cm) were 4.79–10.71%, 6.35–10.78%, 6.27–7.19% and 7.65–7.84% for April, May, June and July, respectively (Table 2). The CVs of the SWCs were 12–22%, 6–23%, 6–11% and 8–9% in the 0–40, 40–120, 120–200 and 200–500 cm soil profile layers, respectively. Therefore, SWC variation was highest in the 0–40 cm soil profile layer throughout the four-month study period. The mean SWC in 200–500 cm soil layer decreased from April to May and then increased into July ($p > 0.05$).

Based on the DSL definition, the upper soil layer (0–100 cm), which was readily affected and replenished by precipitation, could not belong to the DSL. Therefore, the DSL was below a soil depth of 100 cm from April to July 2016, but was present at a soil depth of 100–150 cm from April to May. The DSL was relatively stable in the vertical soil profile.

3.2. Isotopic composition of precipitation, soil water and plant xylem water

Based on multi-year mean monthly weather conditions, we determined that the transition period from the dry to the rainy season defined in this study was feasible (Fig. 4A and B). Monthly variation in $\delta^{18}O$ values for precipitation is shown in Fig. 4C. The $\delta^{18}O$ values decreased from May to July and then increased in August. Therefore, lower $\delta^{18}O$ values were observed during heavy and continuous rainfall events (e.g., July 2016). Moreover, $\delta^{18}O$ values in precipitation ranged from −15.2‰ to 2.3‰, with an average value of −7.23‰, and δD values in precipitation ranged from −111‰ to −16‰, with an average value of −47‰, throughout the observation period (Fig. 5). The linear relationship between $\delta^{18}O$ and δD in rainwater can be expressed as $y = 7.95x + 10.63$, which we determined to be the local meteoric water line (LMWL). The LMWL was below the global meteoric

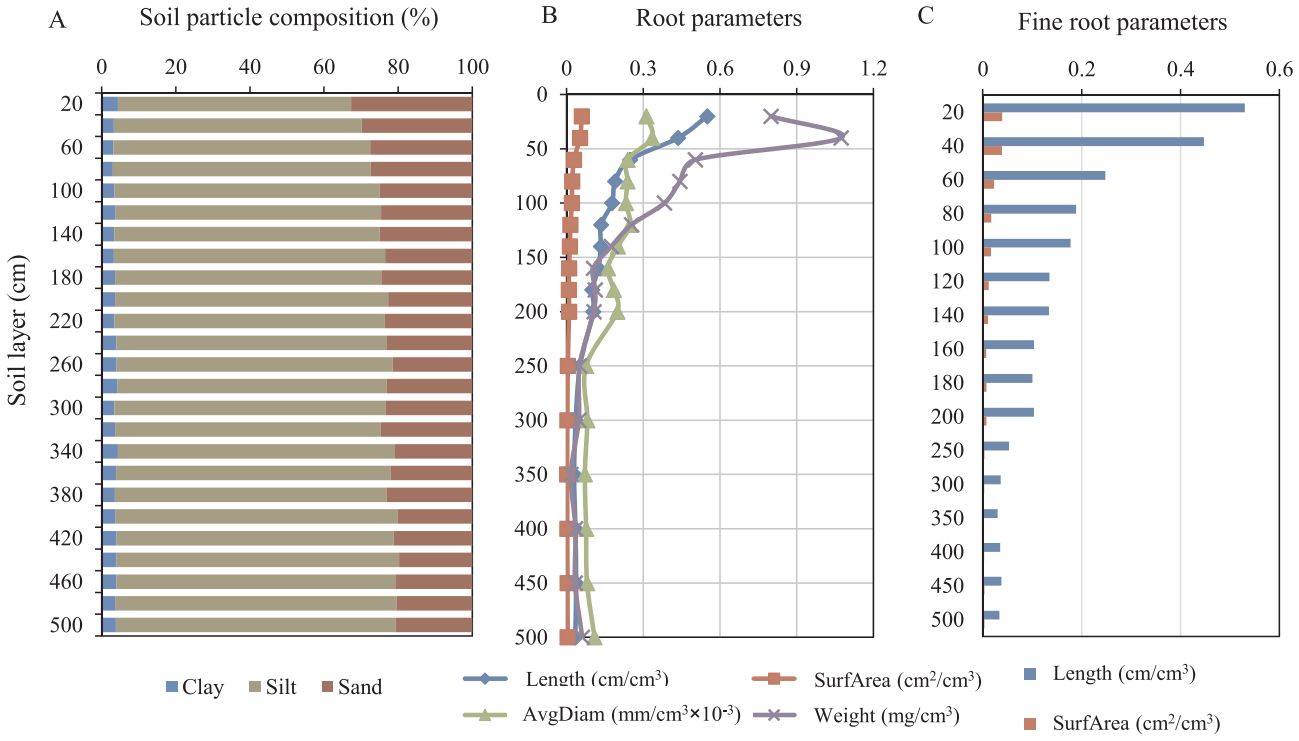

Fig. 2. Distribution of soil particle composition (A), total plant root parameters (B) and fine root parameters (C) of *Robinia pseudoacacia* throughout the 0–500 cm soil profile layer in the sampling site. SurfArea represents surface area; AvgDiam represents average diameter.

water line [GMWL; $\delta D = 8.17\ (\delta^{18}O) + 10.35$] (Rozanski et al., 1993), which we attributed to a weak evaporation effect.

The stable isotopic signatures in soil water ranged from −11.37‰ to −3.99‰ for $\delta^{18}O$ and from −84.17‰ to −36.16‰ for δD throughout the entire soil profile for the four-month study period. The relationship between $\delta^{18}O$ and δD in soil water was $y = 6.39x - 10.17$ (Fig. 5). The mean $\delta^{18}O$ in the 0–40 cm soil profile layer varied from −9.13‰ to −5.84‰ with significant variation throughout the different months, and the mean δD also showed significant variation from −66.02‰ to −46.08‰ (Table 3). Both $\delta^{18}O$ and δD signatures in soil water at different soil depths changed abruptly from month to month, reflecting a rapidly changing dynamic process in soil evaporation and rainfall percolation. The $\delta^{18}O$ and δD values in xylem water varied from −9.17‰ to −3.13‰ and from −67.81‰ to −45.31‰, respectively, during the measurement period. The fitting line of the $\delta^{18}O$ and δD relationship was $y = 3.68x - 31.96$ in xylem water. Interceptions and slopes of soil water and xylem water were less than those for precipitation, which indicated that soil water and xylem water derived from precipitation and there was an evaporation effect on both soil and plant water.

3.3. Potential water sources for plant uptake

Since this tree species cannot directly utilize precipitation and groundwater, being too deep to access (Huang et al., 2013), it may be inferred that soil water was the exclusive source for plant growth. We applied the following two methods to determine when and which soil water layer was utilized by *R. pseudoacacia*. First, we used the direct inference method to investigate the primary soil water sources. In April 2016, $\delta^{18}O$ and δD values in xylem water were similar to those in soil water at 0–40, 40–120 and 200–500 cm soil profile layer depths (Fig. 6). In May, however, $\delta^{18}O$ and δD values in xylem water were close to those in soil water at 0–40 and 40–120 cm soil profile layer depths. As the month progressed, $\delta^{18}O$ and δD values in xylem water were similar to those in soil water at 0–40 and 40–120 cm soil profile layer depths in June 2016. In July, $\delta^{18}O$ and δD values in xylem water matched those in soil water at 0–40 and 200–500 cm soil profile depths.

The proportion of water uptake in the soil profile layers as determined by the MixSIAR model are shown in Fig. 7A. Water sources in the vertical profile showed variation among the four months. In April, *R. pseudoacacia* mainly used soil water in the intermediate-shallow and deep soil layers. In May, the proportion in different soil profile layers fluctuated within the vertical profile except for the 20–250 cm soil profile layer. In June, the water source proportion in all soil profile layers was similar except for the 20–120 cm soil profile layer. In July, the largest water source proportion was mainly distributed within the 0–120 cm soil profile later.

Summarizing results obtained from the MixSIAR model showed that 26.2% and 48.4% of the water used by *R. pseudoacacia* derived from the 40–120 and 200–500 cm soil profile layers, respectively, in April 2016 (Fig. 7B). In May, *R. pseudoacacia* accessed water from the 0–40 cm soil profile layer (21.5%), the 40–120 cm soil profile layer (24.5%) and the 200–500 cm soil profile layer (37.4%). In June and July, 51.6% and 53.6% of the water utilized by *R. pseudoacacia* mainly derived from the 0–120 cm soil profile layer, respectively.

4. Discussion

4.1. Monthly soil water features based on soil water content and stable isotopes

During the transition period from the dry to the rainy season, SWC values changed dramatically in the 0–150 cm soil profile layer from April to July (Fig. 3). Similar trends in seasonal SWC have been reported by other studies (Liang et al., 2018; Chang et al., 2019; Yu et al., 2019; Zhao et al., 2019). This could be attributed to (1) the thawing of the frozen soil layer resulting from increasing temperatures in April and May, and the form of ice will cause high soil water content (Fig. 4A and B); (2) sand content in the 0–100 cm soil profile layer was relatively higher than that in the deeper soil layers, favoring thawing as

Table 1
Statistical data of soil particle composition and plant roots in the four soil profile layers in the study area.

Soil layer (cm)	Parameters	Min	Max	Mean	SD	CV (%)	R (%)
0–40	Clay (%)	3.29	4.37	3.83	0.76	20	
	Silt (%)	62.95	66.86	64.91	2.76	4	
	Sand (%)	29.85	32.69	31.27	2.01	6	
	Length (cm/cm^3)	0.436	0.550	0.493	0.081	16	53
	SurfArea (cm^2/cm^3)	0.053	0.060	0.056	0.005	9	36
	AvgDiam ($mm/cm^3 \times 10^{-3}$)	0.313	0.335	0.324	0.016	5	29
	Weight (mg/cm^3)	0.799	1.074	0.937	0.194	21	55
40–120	Clay (%)	3.04	3.76	3.34	0.32	10	
	Silt (%)	69.33	71.65	70.53	1.26	2	
	Sand (%)	24.64	27.53	26.13	1.55	6	
	Length (cm/cm^3)	0.135	0.249	0.188	0.047	25	31
	SurfArea (cm^2/cm^3)	0.016	0.029	0.022	0.006	27	43
	AvgDiam ($mm/cm^3 \times 10^{-3}$)	0.233	0.249	0.240	0.007	3	13
	Weight (mg/cm^3)	0.255	0.504	0.396	0.107	27	30
120–200	Clay (%)	3.28	3.66	3.49	0.18	5	
	Silt (%)	71.67	73.67	72.61	0.99	1	
	Sand (%)	22.66	24.93	23.90	1.02	4	
	Length (cm/cm^3)	0.101	0.134	0.116	0.016	14	11
	SurfArea (cm^2/cm^3)	0.009	0.013	0.011	0.002	18	14
	AvgDiam ($mm/cm^3 \times 10^{-3}$)	0.162	0.201	0.187	0.018	10	33
	Weight (mg/cm^3)	0.105	0.175	0.125	0.034	27	10
200–500	Clay (%)	3.43	4.39	3.88	0.29	7	
	Silt (%)	71.66	76.21	74.23	1.42	2	
	Sand (%)	19.73	24.68	21.89	1.51	7	
	Length (cm/cm^3)	0.030	0.053	0.038	0.008	21	5
	SurfArea (cm^2/cm^3)	0.003	0.005	0.004	0.001	25	7
	AvgDiam ($mm/cm^3 \times 10^{-3}$)	0.072	0.110	0.083	0.014	17	25
	Weight (mg/cm^3)	0.017	0.062	0.041	0.016	39	5

Note: SD represents stand deviation; SurfArea represents surface area; AvgDiam represents average diameter; R represents the ratio of plant root parameters in the four soil profile layers to the whole profile.

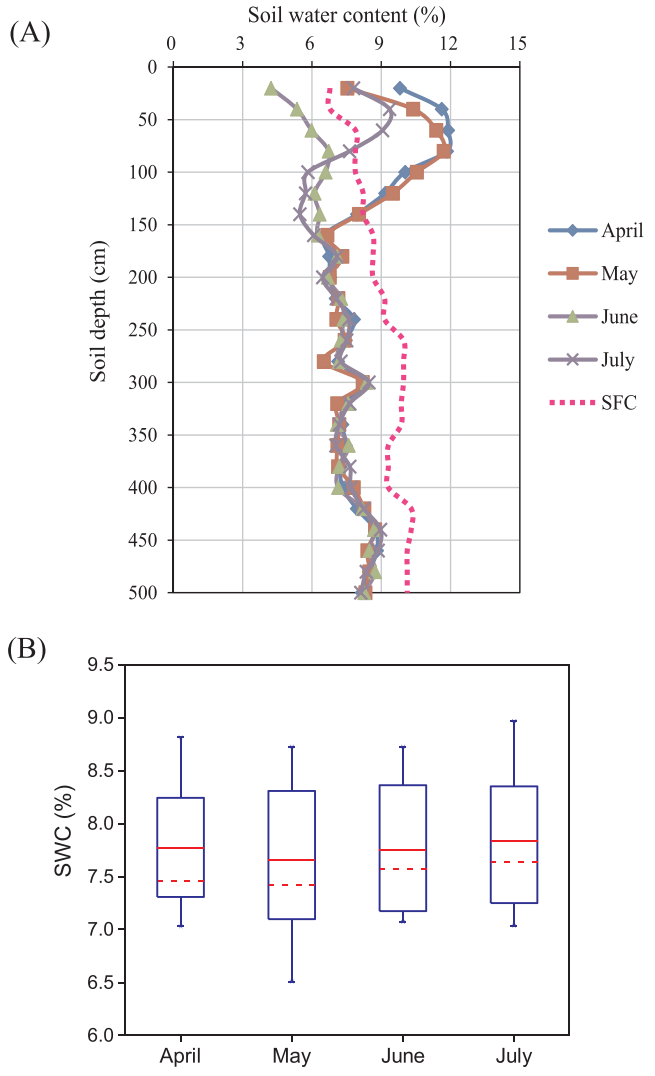

Fig. 3. Vertical distribution of soil water content (SWC) and the stable field capacity (SFC) along the 0–500 cm soil profile in the sampling site (A) and the mean SWCs in the 200–500 cm soil profile layer (B) during the four month study period. The red solid line represents the mean value, the red dashed line represents the median value. (For interpretation of the references to colour in this figure legend, the reader is referred to the web version of this article.)

temperatures increased; (3) a slight decline of SWC due to increasing evaporation and water movement in May; (4) as the months progressed, intensive evaporation and plant uptake caused the lowest SWC to occur in June. However, a large amount of continuous precipitation (i.e., 140.1 mm) occurred on July 8th and July 30th (Fig. 4), which recharged soil water and led to an obvious increase in SWC. Moreover, SWC in the shallow soil layer (0–40 cm) significantly changed during the transition period, while SWC was only weakly influenced by precipitation or evaporation in the deep soil layers (Yang et al., 2012; Li et al., 2015). These deep layers were only affected by infiltration, which were mainly influenced by soil properties and plant roots (Wu et al., 2011; Wang et al., 2013, 2019). Soil particle composition and plant roots were relatively stable in the 200–500 cm soil profile layer in this study (Fig. 2); therefore, SWC did not significantly vary in the deep soil layer.

In the CLP, precipitation is the sole source of soil water, while evaporation is the major factor for the enrichment of isotopes in shallow soil layers (Xue, 1995; Wan and Liu, 2016). Soil water between the surface and a depth of 200 cm showed distinct variation, and the $\delta^{18}O$ and δD profiles changed significantly during the transition period, reflecting both the isotopic ratio of recent precipitation and evaporative fractionation. The distribution of $\delta^{18}O$ in the soil profile in April 2016 also confirmed that the evaporation rate was low during this period compared to other months. However, the depletion in upper soil layers in April may indicate an evaporative front. Since no rainfall event occurred prior to sample collection, the effect of recent precipitation could be excluded. The isotopic profiles in soil water in this study did not always decrease smoothly as reported by Zimmermann et al. (1966) (i.e. July 2016), which means that the isotope composition in soil water is not only affected by evaporation but is also influenced by infiltration. Significant and continuous rainfall events occurred prior to July 26, resulting in a low $\delta^{18}O$ value in the near surface soil layer. Both evaporation and precipitation led to a negative correlation between SWC and the stable isotopes ($\delta^{18}O$ and δD), which was also reported by previous studies (Eggemeyer et al., 2009; Wan and Liu, 2016; Zhu et al., 2018). In addition, vegetation samples had a flatter evaporation line than soil as shown in Fig. 5, which may suggest an independent evaporation process occurring in May and June. However, the trend in the isotopic ratio in soil water in the vertical profile was similar in May and June as shown in Fig. 6, differing from the patterns observed in April and July. MixSIAR modeling results demonstrated that the proportion of water uptake in each soil layer during May and June was homogeneous except for the surface soil layer, which may indicate that independent evaporation processes in vegetation samples have a weak

Table 2
Seasonal variations in soil water content (SWC) in the four soil profile layers.

Soil layer (cm)	Item	Statistics	2016/4	2016/5	2016/6	2016/7
0–40	SWC	Min (%)	9.81	7.53	4.22	7.80
		Max (%)	11.61	10.38	5.35	9.36
		Mean (%)	10.71	8.96	4.79	8.58
		SD	1.28	2.01	0.80	1.10
		CV (%)	12	22	17	13
40–120	SWC	Min (‰)	9.16	9.50	5.97	5.72
		Max (‰)	11.89	11.70	6.72	9.05
		Mean (‰)	10.73	10.78	6.35	7.05
		SD	1.36	0.98	0.36	1.60
		CV (%)	13	9	6	23
120–200	SWC	Min (‰)	6.53	6.66	6.25	5.48
		Max (‰)	7.95	8.04	7.08	7.08
		Mean (‰)	7.00	7.19	6.58	6.27
		SD	0.64	0.63	0.38	0.67
		CV (%)	9	9	6	11
200–500	SWC	Min (‰)	7.03	7.05	7.07	7.03
		Max (‰)	8.82	8.73	8.73	8.97
		Mean (‰)	7.77	7.65	7.75	7.84
		SD	0.59	0.69	0.62	0.63
		CV (%)	8	9	8	8

Note: SD represents stand deviation; CV represents coefficient of variation.

effect on the source inference.

The $\delta^{18}O$ was relatively stable with a mean value of –8.01‰ below a depth of 200 cm, which demonstrates that typical rainfall events and even continuous precipitation (129.9 mm) have less impact on soil water in deep soil layers. The mean $\delta^{18}O$ value in the 200–500 cm soil profile layer was close to the mean $\delta^{18}O$ value of annual precipitation, and local stable isotopes ($\delta^{18}O$ and δD) in precipitation were relatively stable in the vicinity of the LMWL; therefore, it can be inferred that soil water in the 200–500 cm soil profile layer derived from previous rainfall events, which can be referred to as "old water". Previous studies have confirmed that infiltration from precipitation into the unsaturated soil zone occurs very slowly in the CLP (Huang et al., 2013; Tan et al., 2017). Therefore, old water could exist in deep soil for a long period of time, which can subsequently be absorbed by plants.

4.2. Water uptake by Robinia pseudoacacia

There were obvious changes in SWC (Fig. 3) in the 0–200 cm soil profile layer along with seasonal changes in precipitation (Fig. 4B), indicating that soil water sources varied monthly in the study area. Our study found that *R. pseudoacacia* mainly utilized soil water from the 40–120 and 200–500 cm soil profile layers in April because the corresponding $\delta^{18}O$ values in xylem water were similar to soil water from these soil layers (Fig. 6). The following are potential reasons why *R. pseudoacacia* primarily uptakes soil water from deep soil layers: (1) First, both air and soil temperature within the upper soil layer is low at the beginning of growing season (April in the study area), wherein the thickness of seasonal permafrost is approximately 50 cm according to our field investigation. This may significantly increase the water use of *Robinia* within the 200–500 cm soil layer in April given that ice in the upper soil layer cannot be utilized by plants, while the neutron probe used in our study identified this ice as soil water content. This feature is different from a study conducted in another semiarid area (Barbeta et al., 2015), whereby water was available in all soil layers in early spring; thus, it is not necessary for tree to uptake water from deep soil layers, and water uptake from deep soil layers increases as the dry summer season progresses. These differences indicated the distinct climatic condition of our area. (2) Physiologically, plant activity in April is weak, and even a small amount of water uptake in soil within the 200–500 cm soil profile layer would result in a relatively high proportion of total water use during this month. (3) The mean soil

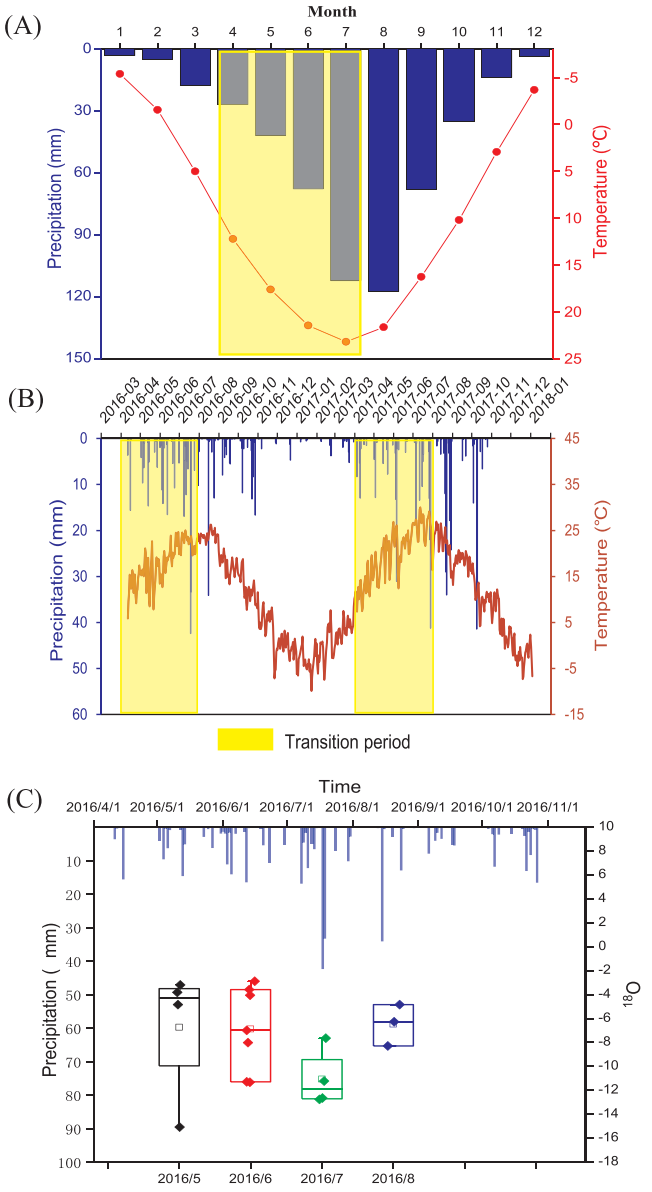

Fig. 4. Multi-year mean monthly precipitation and temperature from 1960 to 2015 obtained from the Yan'an meteorological station (A), weather conditions near our sampling site (B) and the stable oxygen isotopes in rain water (C) in the Guntun watershed during the study period. Yellow shaded areas denote the transition period from the dry to the rainy season. Blue represents precipitation, red represents temperature. Error bars in (C) represent standard deviation. (For interpretation of the references to colour in this figure legend, the reader is referred to the web version of this article.)

water content was calculated in the 200–500 cm soil layer, and results are provided in Fig. 3B. The mean soil water content decreased from April to May, which verified the water-use strategy of deep roots. A similar phenomenon was reported in a previous study (Asbjornsen et al., 2007); however, the soil sampling depth in that study was limited to 200 cm. With an increase in air and soil temperatures, the proportion of water uptake in the shallow soil layers increased in May. Also, in June, the 0–40 and 40–120 cm soil profile layers yielded the highest overall ratios. This could be attributed to the recharge of a small quantity of precipitation to soil water which ultimately provided enough water for the species to use. In July, *R. pseudoacacia* mainly utilized soil water from the 40–120 cm soil profile layer, which could be attributable to the significant and continuous precipitation that occurred before sample collection. In addition, a previous study showed

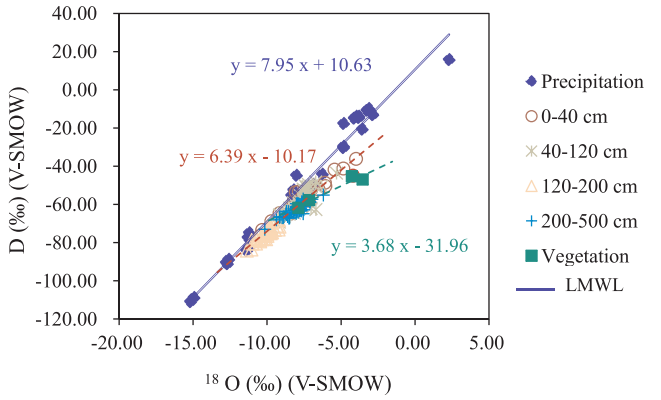

Fig. 5. Relationships between δD and $\delta^{18}O$ signatures in rainwater, soil water and xylem water of *Robinia pseudoacacia* from April to August 2016. The local meteoric water line (y = 7.95x + 10.63), the soil water line (y = 6.39x − 10.17) and the twig xylem water line (y = 3.68x − 31.96) are also shown.

Table 3
Seasonal variation of stable isotopes ($\delta^{18}O$ and δD) in the four soil profile layers.

Soil layer (cm)	Item	Statistics	2016/4	2016/5	2016/6	2016/7
0–40	$\delta^{18}O$	Min (‰)	−9.16	−7.82	−6.93	−10.16
		Max (‰)	−8.37	−5.76	−4.76	−8.10
		Mean (‰)	−8.76	−6.79	−5.84	−9.13
		SD	0.56	1.46	1.54	1.45
	δD	Min (%)	−64.78	−53.42	−52.42	−72.86
		Max (%)	−64.70	−48.58	−39.74	−59.17
		Mean (%)	−64.74	−51.00	−46.08	−66.02
		SD	0.06	3.42	8.96	9.68
40–120	$\delta^{18}O$	Min (%)	−9.06	−8.89	−9.13	−9.36
		Max (%)	−6.65	−7.05	−7.50	−7.32
		Mean (%)	−7.97	−7.74	−8.18	−8.26
		SD	1.02	0.86	0.77	0.92
	δD	Min (‰)	−67.53	−65.30	−68.83	−69.81
		Max (‰)	−50.86	−49.60	−53.29	−54.35
		Mean (‰)	−60.01	−56.41	−60.14	−61.47
		SD	6.97	7.09	7.02	7.24
120–200	$\delta^{18}O$	Min (%)	−10.03	−10.70	−10.04	−10.80
		Max (%)	−9.77	−9.57	−9.68	−9.94
		Mean (%)	−9.85	−10.29	−9.86	−10.30
		SD	0.12	0.50	0.17	0.43
	δD	Min (%)	−77.07	−79.51	−76.01	−79.58
		Max (%)	−71.94	–71.21	−71.65	−73.20
		Mean (%)	−74.87	−76.07	−73.91	−76.19
		SD	2.16	3.55	2.07	2.98
200–500	$\delta^{18}O$	Min (%)	−7.95	−9.03	−9.01	−8.62
		Max (%)	−7.00	−7.78	−7.62	−7.66
		Mean (%)	−7.51	−8.25	−8.13	−8.14
		SD	0.35	0.43	0.49	0.38
	δD	Min (%)	−62.97	−66.15	−66.15	−67.18
		Max (%)	−58.35	−61.45	−59.88	−59.77
		Mean (%)	−61.32	−63.04	−62.38	−63.65
		SD	2.09	1.75	2.27	2.80

Note: SD represents stand deviation.

that response depth to precipitation was within the top 200 cm in the CLP (Fu et al., 2018). Therefore, the water uptake pattern in July was mainly influenced by initial periods and instantaneous precipitation events.

The water utilization characteristics employed by *R. pseudoacacia* during the transition period from April to July showed obvious variation. Throughout the study period, the trend in water uptake from the shallow soil profile layer (0–40 cm) and the intermediate-shallow soil profile layer (40–120 cm) increased; while the trend in water uptake from the deep soil profile layer (200–500 cm) decreased. Characteristics of the species' water uptake feature among the different soil layers during the transition period indicated that the water source of this tree species is affected by significant variation in the external climate and the internal soil environment. This could have resulted from (1) an increase in precipitation wherein rainwater infiltrated into the shallow and intermediate-shallow soil profile layers; (2) the species gradually entering into its vigorous growth state, which would significantly increase its water demand; (3) root uptake of deep soil water to support tree growth and nutrient absorption during the dry season, which is similar to results from Nie et al. (2012) who reported that *R. pseudoacacia* tended to use deep soil water during the latter part of the dry season. Therefore, the way by which *R. pseudoacacia* uptakes soil water is dependent on variables such as water availability, plant growth and root distribution (Zhu et al., 2018).

Root distribution patterns affect plant water-use strategies and nutrient absorption. Huo et al. (2018) found that different aged jujube trees exhibited different water uptake patterns closely correlated to root distribution. They reported that the fine root length density of 4- and 8-yr old jujube trees at a depth of 0–60 cm was 90.00% and 62.90%, respectively; therefore, 8-yr old jujube trees are predisposed to use deep soil water. Similar results have also been shown by other studies (Bouillet et al., 2002; Li et al., 2017). In our study, *R. pseudoacacia* roots were measured at a depth of 500 cm. Although root biomass was predominately distributed in the shallow and intermediate-shallow soil profile layers, roots in the deep soil profile layer may play an important role in regulating its water-use strategy. Moreover, to the best of our knowledge, previous studies in the CLP only collected soil samples at a depth of approximately 200 cm (mostly < 100 cm); therefore, stable isotope ($\delta^{18}O$ and δD) regimes below a 200 cm depth remain largely unknown (Wan and Liu, 2016; Huo et al., 2018). Furthermore, plants cannot access deep water sources (such as groundwater) in this region (Huang et al., 2013; Tan et al., 2017); therefore, using deep soil water is an alternative choice for plants in resisting periods of water stress (e.g., extremely dry periods). Our study provides new evidence that plants to indeed use water sources in the deep soil layer in the CLP. Understanding the water-use strategy of the dominant tree species in the CLP is very important for understanding water cycle mechanisms in the soil-plant-atmosphere system to manage water resources and to regulate ecosystem functions for both researchers and policymakers.

4.3. Relationship between the water uptake pattern and the dried soil layer of *Robinia pseudoacacia*

The formation of the DSL constitutes a unique hydrological phenomenon occurring in the CLP, which is mainly caused by the excessive depletion of deep soil water by both native and non-native vegetation, high evapotranspiration and insufficient long-term rainwater supplies (Jipp et al., 1998; Shangguan, 2007; Chen et al., 2008b). A DSL is always located at a certain soil depth, primarily in deep layers that may extend to 10 m below the soil surface (Wang et al., 2010, 2011). The occurrence of DSLs hinders and disrupts the water cycle in the soil–-plant-atmosphere system, which in turn has a negative impact on the development of vegetation.

The implementation of the Grain for Green program in 1999 under the auspice of the Government of China has dramatically changed the landscape of the CLP, doubling the vegetation coverage in the last 16 yr (Chen et al., 2015). It is important to note that *R. pseudoacacia* was initially planted on a large scale (Jian et al., 2015). Moreover, this species was able to successfully adapt to the environment by utilizing deep soil water and has subsequently become the dominant tree species in the CLP. Previous studies have shown that *R. pseudoacacia* uptakes more water than shrubland, grassland and cropland species (Wang et al., 2011, 2015).

Our results demonstrated that *R. pseudoacacia* does in fact use deep soil water layers (200–500 cm) where the DSL has developed during the dry season. The formation of a DSL depends on the soil-water balance

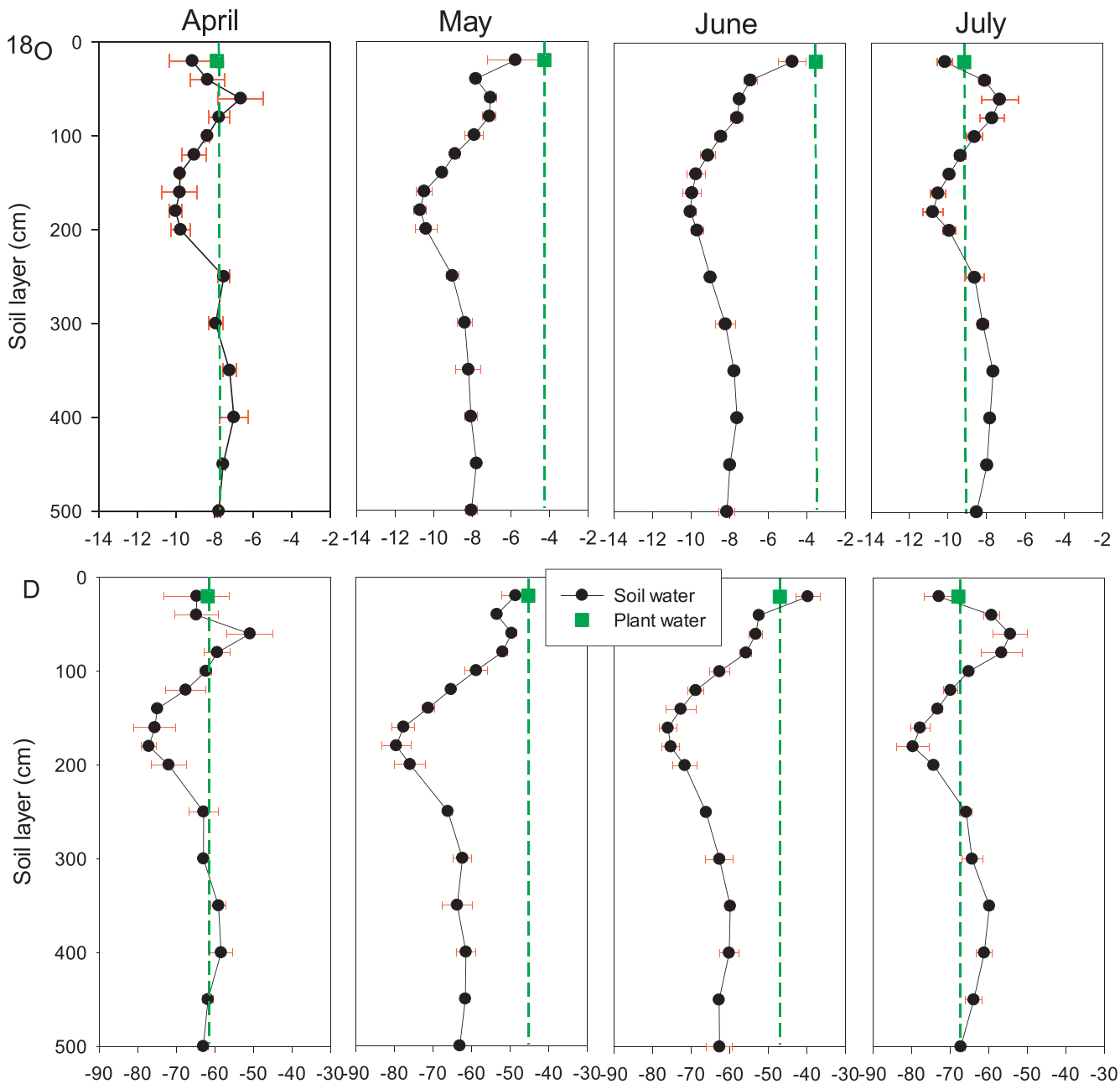

Fig. 6. Seasonal variation in δD and $\delta^{18}O$ signatures in xylem and soil (0–500 cm) water during the study period. Error bars represent stand deviation.

and water cycles of an ecosystem. Generally, when soil-water outputs such as evapotranspiration, drainage and water use increase or soil-water inputs such as rainfall or irrigation decrease, soil drying may occur, and a DSL may form. Therefore, the formation of a DSL is a combined process associated with environmental factors: (1) low rainfall; (2) high evapotranspiration; (3) the large soil water demand of vegetation, and water being prevented from infiltrating into the deep soil layer. Although the DSL formed prior to sampling, characteristics of water uptake during the transition period from the dry to the rainy season aggravated the evolution of the DSL. After the formation of a DSL, continued water uptake from *R. pseudoacacia* would further decrease the SWC within the DSL, which in turn could aggravate the development of the DSL. Thus, the formation of a DSL is an issue of water balance coupled with the fact that trees can access water in deep soil layers in spring when it remains unavailable in surface soil layers. Therefore, data on *R. pseudoacacia* water use during this transition period is of critical importance in understanding the evolution of DSLs.

Studies have pointed out that DSLs will change temporally depending on water replenishment (Chen et al., 2008b; Wang et al., 2011). Because *R. pseudoacacia* can utilize deep soil water during the dry season and during typical years, deep soil water cannot be replenished by precipitation over the short-term; therefore, seasonal water uptake patterns may accelerate the extent of DSL thickness (which should be further investigated due to the 500 cm sample depth limit of this study) and aggravate DSL soil water deficits. A severe DSL would result in long-term adverse effects to plants, leading to the occurrence of what is known as “little old trees” that gradually die, which is detrimental to ecological environment restoration. Therefore, understanding water-use mechanisms of deep plant roots and the evolution of DSLs is crucial for plant management regarding the sustainable utilization of limited water resources. The selection of plant species and planting densities should therefore be taken into account during re-vegetation processes.

Applying the stable isotope ($\delta^{18}O$ and δD) technique not only

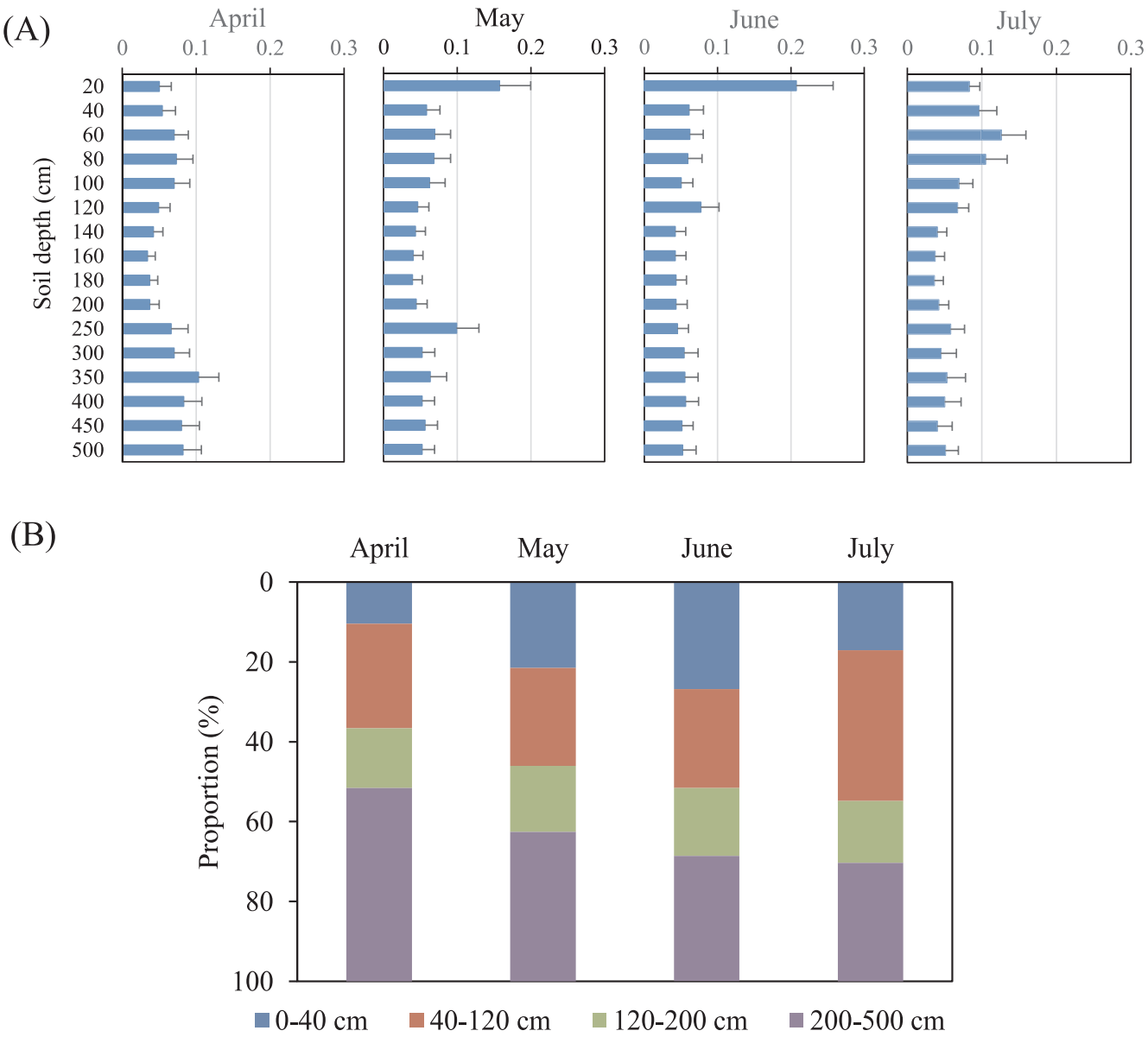

Fig. 7. The water uptake proportion in the soil profile layers from the MixSIAR model (A) and seasonal variation in the proportion of water uptake from the four soil layers (B) that *Robinia pseudoacacia* utilized during different months. Error bars represent standard deviation.

reveals the water sources used by plants but also provides new insight into ecological environment problems associated with local ecosystems. For example, Song et al. (2016a,b) utilized $\delta^{18}O$ and δD signatures to explain why Mongolian Scots pine (*Pinus sylvestris* var. *mongolica*) mortality has increased in recent years. In our study, we determined that the water uptake strategy of deep plant roots during the dry season will exacerbate the status of DSLs, while a decrease in SWC within DSLs will conversely threaten plant growth. Further studies should also be conducted to investigate the relationship between DSL evolution and the water uptake mechanisms of plants in the CLP. Specifically, detailed information on water utilization characteristics during the dry season or throughout the entire year should be ascertained in order to understand DSL development processes.

5. Conclusions

This study used stable isotopes ($\delta^{18}O$ and δD) to reveal the dynamic water uptake patterns of *R. pseudoacacia* during the transition period from the dry to the rainy season in the CLP. Plant roots were mainly distributed within the 0–120 cm soil layer. The SWC and the stable isotope signatures in the upper soil layers showed significant variation over the four-month study period. Moreover, $\delta^{18}O$ and δD signatures in precipitation, soil water and plant water exhibited an apparent correlation during the study period. The water uptake strategy of *R. pseudoacacia* was to switch between the different soil layers from April to July. This tree species mainly utilized soil water from the 40–120 and the 200–500 cm soil layer profiles in April, from the 0–40, 40–120 and 200–500 cm soil layer profiles in May, and from the 0–120 cm soil layer profile in June and July. This closely correlated to precipitation and plant root distribution. Results of *R. pseudoacacia* water-use characteristics obtained by this study provide information concerning the relationship between plant water uptake strategies and the development of DSLs in the CLP.

Declaration of Competing Interest

The authors declare that they have no known competing financial interests or personal relationships that could have appeared to

influence the work reported in this paper.

Acknowledgements

This study was supported by the National Natural Science Foundation of China (Nos. 41722106, 41530854, and 41471189) and the "Ten Thousand Talent Program" for Young Top-Notch Talent. We appreciate the editor of the journal and the reviewers for their useful comments and suggestions of this draft. We acknowledge the effort of Mr. Brian Doonan for improving the manuscript. Special thanks also go to the Gutun station for providing field support toward on this study.

References

Asbjornsen, H., Mora, G., Helmers, M.J., 2007. Variation in water uptake dynamics among contrasting agricultural and native plant communities in the Midwestern U.S. Agric. Ecosyst. Environ. 121, 343–356.
Asbjornsen, H., Shepherd, G., Helmers, M., Mora, G., 2008. Seasonal patterns in depth of water uptake under contrasting annual and perennial systems in the Corn Belt Region of the Midwestern U.S. Plant Soil 308, 69–92.
Barbeta, A., Mejía Chang, M., Ogaya, R., Voltas, J., Dawson, T.E., Peñuelas, J., 2015. The combined effects of a long-term experimental drought and an extreme drought on the use of plant-water sources in a Mediterranean forest. Glob. Change Biol. 21, 1213–1225.
Bouillet, J.P., Laclau, J.P., Arnaud, M., M'Bou, A.T., Saint André, L., Jourdan, C., 2002. Changes with age in the spatial distribution of roots of *Eucalyptus* clone in Congo: impact on water and nutrient uptake. For. Ecol. Manage. 171, 43–57.
Chang, E., Li, P., Li, Z., Xiao, L., Zhao, B., Su, Y., Feng, Z., 2019. Using water isotopes to analyze water uptake during vegetation succession on abandoned cropland on the Loess Plateau, China. Catena 181, 104095.
Chen, H.S., Shao, M.A., Li, Y.Y., 2008a. The characteristics of soil water cycle and water balance on steep grassland under natural and simulated rainfall conditions in the Loess Plateau of China. J. Hydrol. 360, 242–251.
Chen, H.S., Shao, M.A., Li, Y.Y., 2008b. Soil desiccation in the Loess Plateau of China. Geoderma 143, 91–100.
Chen, Y.P., Wang, K.B., Lin, Y.S., Shi, W.Y., Song, Y., He, X.H., 2015. Balancing green and grain trade. Nat. Geosci. 8, 739–741.
Corbin, J.D., Thomsen, M.A., Dawson, T.E., D'Antonio, C.M., 2005. Summer water use by California coastal prairie grasses: fog, drought, and community composition. Oecologia 145, 511–521.
Dai, Y., Zheng, X.J., Tang, L.S., Li, Y., 2015. Stable oxygen isotopes reveal distinct water use patterns of two Haloxylon species in the Gurbantonggut Desert. Plant Soil 389, 73–87.
Eggemeyer, K.D., Awada, T., Harvey, F.E., Wedin, D.A., Zhou, X., Zanner, C.W., 2009. Seasonal changes in depth of water uptake for encroaching trees *Juniperus virginiana* and *Pinus ponderosa* and two dominant C4 grasses in a semiarid grassland. Tree Physiol. 29, 157–169.
Ehleringer, J.R., Dawson, T.E., 1992. Water uptake by plants: perspectives from stable isotope composition. Plant, Cell Environ. 15, 1073–1082.
Ellsworth, P.Z., Williams, D.G., 2007. Hydrogen isotope fractionation during water uptake by woody xerophytes. Plant Soil 291, 93–107.
Fu, Z.H., Wang, Y.Q., An, Z.S., Hu, W., Mostofa, K.M.G., Li, X.Z., Liu, B.X., 2018. Spatial and temporal variability of 0- to 5-m soil–water storage at the watershed scale. Hydrol. Process. 32, 2557–2569.
House, J.I., Archer, S., Breshears, D.D., Scholes, R.J., 2003. Conundrums in mixed woody–herbaceous plant systems. J. Biogeogr. 30, 1763–1777.
Huang, T.M., Pang, Z.H., Yuan, L.J., 2013. Nitrate in groundwater and the unsaturated zone in (semi) arid northern China: baseline and factors controlling its transport and fate. Environ. Earth Sci. 70, 145–156.
Huo, G.P., Zhao, X.N., Gao, X.D., Wang, S.F., Pan, Y. H., 2018. Seasonal water use patterns of rainfed *jujube* trees in stands of different ages under semiarid Plantations in China. Agric. Ecosyst. Environ. 265, 392–401.
Jian, S.Q., Zhao, C.Y., Fang, S.M., Yu, K., 2015. Effects of different vegetation restoration on soil water storage and water balance in the Chinese Loess Plateau. Agric. For. Meteorol. 206, 85–96.
Jipp, P.H., Nepstad, D.C., Cassel, D., De Carvalho, C.R., 1998. Deep soil moisture storage and transpiration in forests and pastures of seasonally-dry Amazonia. In: Potential Impacts of Climate Change on Tropical Forest Ecosystems. Springer, pp. 255–272.
Kerhoulas, L.P., Kolb, T.E., Koch, G.W., 2013. Tree size, stand density, and the source of water used across seasons by ponderosa pine in northern Arizona. For. Ecol. Manage. 289, 425–433.
Leo, M., Oberhuber, W., Schuster, R., Grams, T.E.E., Matyssek, R., Wieser, G., 2014. Evaluating the effect of plant water availability on inner alpine coniferous trees based on sap flow measurements. Eur. J. Forest Res. 133, 691–698.
Li, H., Si, B., Li, M., 2018. Rooting depth controls potential groundwater recharge on hillslopes. J. Hydrol. 564, 164–174.
Li, L.S., Gao, X.D., Wu, P.T., Zhao, X.N., Li, H.C., Ling, Q., Sun, W.H., 2017. Soil water content and root patterns in a rain-fed *Jujube* plantation across stand ages on the Loess Plateau of China. Land Degrad. Dev. 28, 207–216.
Li, S.G., Romero Saltos, H., Tsujimura, M., Sugimoto, A., Sasaki, L., Davaa, G., Oyunbaatar, D., 2007. Plant water sources in the cold semiarid ecosystem of the upper Kherlen River catchment in Mongolia: a stable isotope approach. J. Hydrol. 333, 109–117.
Li, X.Z., Shao, M.A., Jia, X.X., Wei, X.R., He, L., 2015. Depth persistence of the spatial pattern of soil–water storage along a small transect in the Loess Plateau of China. J. Hydrol. 529 (Part 3), 685–695.
Liang, H., Xue, Y., Shi, J., Li, Z., Liu, G., Fu, B., 2018. Soil moisture dynamics under *Caragana korshinskii* shrubs of different ages in Wuzhai County on the Loess Plateau, China. Earth Environ. Sci. Trans. R. Soc. Edinburgh 109, 387–396.
Lubis, M.E.S., Harahap, I.Y., Hidayat, T.C., Pangaribuan, Y., Sutarta, E.S., Rahman, Z.A., Teh, C., Hanafi, M., 2014. Stable oxygen and deuterium isotope techniques to identify plant water sources. J. Water Resour. Prot. 6, 1501–1508.
Matzner, S.L., Rice, K.J., Richards, J.H., 2003. Patterns of stomatal conductance among blue oak (*Quercus douglasii*) size classes and populations: implications for seedling establishment. Tree Physiol. 23, 777–784.
Nie, Y.P., Chen, H.S., Wang, K.L., Tan, W., Deng, P.Y., Yang, J., 2011. Seasonal water use patterns of woody species growing on the continuous dolostone outcrops and nearby thin soils in subtropical China. Plant Soil 341, 399–412.
Nie, Y.P., Chen, H.S., Wang, K.L., Yang, J., 2012. Water source utilization by woody plants growing on dolomite outcrops and nearby soils during dry seasons in karst region of Southwest China. J. Hydrol. 420, 264–274.
Parnell, A.C., Phillips, D.L., Bearhop, S., Semmens, B.X., Ward, E.J., Moore, J.W., Jackson, A.L., Grey, J., Kelly, D.J., Inger, R., 2013. Bayesian stable isotope mixing models. Environmetrics 24, 387–399.
Rozanski, K., Araguás-Araguás, L., Gonfiantini, R., 1993. Isotopic patterns in modern global precipitation. Clim. Change Continental Isotopic Rec. 1–36.
Sala, O.E., Golluscio, R.A., Lauenroth, W.K., Soriano, A., 1989. Resource partitioning between shrubs and grasses in the Patagonian steppe. Oecologia 81, 501–505.
Scholes, R.J., Archer, S.R., 1997. Tree-grass interactions in savannas. Annu. Rev. Ecol. Syst. 28, 517–544.
Schultz, N.M., Griffis, T.J., Lee, X., Baker, J.M., 2011. Identification and correction of spectral contamination in 2H/1H and 18O/16O measured in leaf, stem, and soil water. Rapid Commun. Mass Spectrosc. 25, 3360–3368.
Schuur, E.A.G., Bockheim, J., Canadell, J.G., Euskirchen, E., Field, C.B., Goryachkin, S.V., Hagemann, S., Kuhry, P., Lafleur, P.M., Lee, H., Mazhitova, G., Nelson, F.E., Rinke, A., Romanovsky, V.E., Shiklomanov, N., Tarnocai, C., Venevsky, S., Vogel, J.G., Zimov, S.A., 2008. Vulnerability of permafrost carbon to climate change: implications for the global carbon cycle. Bioscience 58, 701–714.
Shangguan, Z.P., 2007. Soil desiccation occurrence an its impact on forest vegetation in the Loess Plateau of China. Int. J. Sust. Dev. World 14, 299–306.
Song, L.N., Zhu, J.J., Li, M.C., Zhang, J.X., 2016a. Water use patterns of *Pinus sylvestris* var. *mongolica* trees of different ages in a semiarid sandy lands of Northeast China. Environ. Exp. Bot. 129, 94–107.
Song, L.N., Zhu, J.J., Li, M.C., Zhang, J.X., Lv, L.Y., 2016b. Sources of water used by *Pinus sylvestris* var. *mongolica* trees based on stable isotope measurements in a semiarid sandy region of Northeast China. Agric. Water Manage. 164, 281–290.
Su, H., Li, Y., Liu, W., Xu, H., Sun, O.J., 2014. Changes in water use with growth in *Ulmus pumila* in semiarid sandy land of northern China. Trees 28, 41–52.
Tan, H.B., Liu, Z.H., Rao, W.B., Wei, H.Z., Zhang, Y.D., Jin, B., 2017. Stable isotopes of soil water: implications for soil water and shallow groundwater recharge in hill and gully regions of the Loess Plateau, China. Agric. Ecosyst. Environ. 243, 1–9.
Walker, B.H., Ludwig, D., Holling, C.S., Peterman, R.M., 1981. Stability of semi-arid savanna grazing systems. J. Ecol. 69, 473–498.
Wan, H., Liu, W.G., 2016. An isotope study (δ18O and δD) of water movements on the Loess Plateau of China in arid and semiarid climates. Ecol. Eng. 93, 226–233.
Wang, L., Wang, Q.J., Wei, S.P., Shao, M.A., Yi, L., 2008. Soil desiccation for Loess soils on natural and regrown areas. For. Ecol. Manage. 255, 2467–2477.
Wang, Y.Q., Shao, M.A., Liu, Z.P., 2013. Vertical distribution and influencing factors of soil water content within 21-m profile on the Chinese Loess Plateau. Geoderma 193, 300–310.
Wang, Y.Q., Shao, M.A., Shao, H.B., 2010. A preliminary investigation of the dynamic characteristics of dried soil layers on the Loess Plateau of China. J. Hydrol. 381, 9–17.
Wang, Y.Q., Shao, M.A., Zhang, C.C., Han, X.W., Mao, T.X., Jia, X.X., 2015. Choosing an optimal land-use pattern for restoring eco-environments in a semiarid region of the Chinese Loess Plateau. Ecol. Eng. 74, 213–222.
Wang, Y.Q., Shao, M.A., Zhu, Y.J., Liu, Z.P., 2011. Impacts of land use and plant characteristics on dried soil layers in different climatic regions on the Loess Plateau of China. Agric. For. Meteorol. 151, 437–448.
Wang, Y.Q., Shao, M.A., Zhu, Y.J., Sun, H., Fang, L.C., 2018. A new index to quantify dried soil layers in water-limited ecosystems: a case study on the Chinese Loess Plateau. Geoderma 322, 1–11.
Wang, Y.Q., Sun, H., Zhao, Y.L., 2019. Characterizing spatial-temporal patterns and abrupt changes in deep soil moisture across an intensively managed watershed. Geoderma 341, 181–194.
Wesche, K., Walther, D., von Wehrden, H., Hensen, I., 2011. Trees in the desert: Reproduction and genetic structure of fragmented *Ulmus pumila* forests in Mongolian drylands. Flora – Morphol. Distrib. Funct. Ecol. Plants 206, 91–99.
Wu, J.E., Liu, W.J., Chen, C.F., 2017. How do plants share water sources in a rubber-tea agroforestry system during the pronounced dry season? Agric. Ecosyst. Environ. 236, 69–77.
Wu, T.N., Wang, Y.Q., Lv, J.W., Zhang, B., 2011. Soil water characteristics of Middle Pleistocene paleosol layers on the loess Plateau. Afr. J. Biotechnol. 10, 10856–10863.
Xue, G., 1995. The mechanism of recharge and occurrence of the groundwater in loess areas. Hydrogeol. Eng. Geol 1, 38–56.
Yang, L., Wei, W., Chen, L.D., Mo, B.R., 2012. Response of deep soil moisture to land use and afforestation in the semi-arid Loess Plateau, China. J. Hydrol. 475, 111–122.
Yang, S.L., Gao, R.L., 1998. Construction of policies and laws for soil and water

conservation in China. In: Proceedings of the International Symposium on Comprehensive Watershed Management (Iswm-'98). pp. 140–144.
Yu, B., Liu, G., Liu, Q., Huang, C., Li, H., Zhao, Z., 2019. Seasonal variation of deep soil moisture under different land uses on the semi-arid Loess Plateau of China. J. Soil Sedim. 19, 1179–1189.
Zhang, K.R., Dang, H.S., Tan, S.D., Wang, Z.X., Zhang, Q.F., 2010. Vegetation community and soil characteristics of abandoned agricultural land and pine plantation in the Qinling Mountains, China. For. Ecol. Manage. 259, 2036–2047.
Zhao, Y.L., Wang, Y.Q., Sun, H., Lin, H., Jin, Z., He, M.N., Yu, Y.L., Zhou, W.J., An, Z.S., 2019. Intensive land restoration profoundly alters the spatial and seasonal patterns of deep soil water storage at watershed scales. Agric. Ecosyst. Environ. 280, 129–141.
Zhu, J.F., Liu, J.T., Lu, Z.H., Li, J.S., Sun, J.K., 2018. Water-use strategies of coexisting shrub species in the Yellow River Delta, China. Can. J. For. Res. 48, 1099–1107.
Zimmermann, U., Münnich, K., Roether, W., Kreutz, W., Schubach, K., Siegel, O., 1966. Tracers determine movement of soil moisture and evapotranspiration. Science 152, 346–347.